ISSN 1070-3284, Russian Journal of Coordination Chemistry, 2021, Vol. 47, No. 6, pp. 365–375. © Pleiades Publishing, Ltd., 2021.
Russian Text © The Author(s), 2021, published in Koordinatsionnaya Khimiya, 2021, Vol. 47, No. 6, pp. 327–337.

New Low-Dimensional Perovskites Based on Lead Bromide

K. L. Isakovskaya[a, b], I. A. Nikovskii[a], and Yu. V. Nelyubina[a, c, *]

[a] *Nesmeyanov Institute of Organoelement Compounds, Russian Academy of Sciences, Moscow, 119991 Russia*
[b] *Mendeleev University of Chemical Technology of Russia, Moscow, 125047 Russia*
[c] *Bauman State Technical University, Moscow, 107005 Russia*
**e-mail: unelya@ineos.ac.ru*

Received December 1, 2020; revised January 19, 2021; accepted January 19, 2021

Abstract—The reactions of lead bromide with 7,7,8,8-tetracyanoquinodimethane and anthracen-9-ylmethanamine hydrobromide in dimethylformamide (DMF) afford the known low-dimensional perovskite $\{PbBr_2(DMF)\}_n$ (**I**) with an impurity of a new hybrid 1D perovskite $\{Ca(DMF)_6[PbBr_3]_2\}_n$ (**II**), which is isolated in the individual form and characterized by X-ray diffraction analysis. In the crystal of compound **II**, lead bromide forms infinite chains of $PbBr_5$ octahedra with one vacant vertex between which calcium cations coordinated by the DMF molecules are arranged. The calcium cations presumably have got into the reaction mixture from water used for the washing of the reaction vessel for crystallization after the previous attempt of the synthesis. An attempt of the purposeful preparation of this hybrid 1D perovskite from various calcium salts as sources of this metal ion gives one more new low-dimensional perovskite $\{Ca(DMF)_6[PbBr_{2.3}Cl_{0.7}]_2\}_n$ (**III**) in which halide anions (bromide and chloride anions from lead bromide and calcium chloride, respectively) build up the coordination sphere of the lead ion to an octahedral one inducing no noticeable changes in the crystal packing compared to that of compound **II**. The X-ray diffraction results are deposited with the Cambridge Crystallographic Data Centre (CIF files CCDC nos. 2045586 (**I**), 2047219 (**II**), and 2047220 (**III**)).

Keywords: lead bromide, hybrid perovskites, low-dimensional perovskites, perovskite-like materials, X-ray diffraction analysis, solar cells

DOI: 10.1134/S1070328421060026

INTRODUCTION

One of the most impressive achievements of the recent years in the area of renewable power sources is related to the fabrication of hybrid perovskite semiconductors [1, 2] of the general formula AMX_3, where M is the metal ion (Pb^{2+} and Sn^{2+}), X is the halide anion (I^-, Br^-, or Cl^-), and A is the organic cation (e.g., $CH_3NH_3^+$ or $NH_2CHNH_2^+$). The optoelectronic characteristics of these materials in which the MX_6 octahedra form a three-dimensional crystal structure are comparable with crystalline silicon that is actively used in modern solar cells. Their main drawback preventing the further development of the related technology [3] is a low stability of hybrid perovskites, which easily decompose under the action of air oxygen and moisture, high temperatures, and even prolonged solar irradiation.

In the recent time, researchers in chemistry and materials science all over the world consider the use of the so-called "low-dimensional" hybrid perovskites as one of solutions of this problem [3–8]. In the hybrid perovskites, octahedra MX_6 (or pyramids MX_5 [9] and tetrahedra MX_4 [10]) form a crystal structure of a lower dimensionality due to which they are more stable [11, 12] than the described above traditional 3D perovskites. In addition, broader opportunities for choosing the organic cation [13], which now should not satisfy rigid requirements imposed on the size [14, 15], make it possible to purposefully prepare 2D [16–20], 1D [21–23], or even 0D perovskites [9, 23, 24] (or perovskite-like materials) with diverse optoelectronic properties that are restricted at the moment only by the use of inert organic cations. The further improvement of the indicated properties, which are insufficient yet for the practical use of low-dimensional perovskites in solar cells [25], with retention of the neces-

sary stability of the material is possible by the replacement of inert organic cations by electroactive conjugated molecules [26]. Polyaromatic compounds (e.g., pyrene [27, 28]) have recently been proposed as such molecules, since they are capable of forming charge-transfer complexes [27–30] with diverse organic acceptors [31, 32]. A doubtless advantage of similar organic–inorganic materials is the possibility of "fine tuning" of their optoelectronic properties using various combinations of the donor and acceptor [31, 32], providing wide prospects of the directed design of new perovskite materials for modern solar cells.

For this purpose, we synthesized anthracen-9-ylmethanamine hydrobromide containing the ammonium group, which should provide binding with the inorganic moiety of hybrid 1D [28] or 2D perovskite [27] based on lead bromide by strong hydrogen bonds N–H...Br, and the presence of the anthracene moiety should provide the formation of a charge-transfer complex with an appropriate organic acceptor. However, its subsequent interaction with lead bromide and 7,7,8,8-tetracyanoquinodimethane, which is one of the most popular acceptors, in DMF unexpectedly gave the well-known compound $\{PbBr_2(DMF)\}_n$ (**I**). Compound **I** was isolated in the individual state and characterized by elemental analysis and X-ray diffraction analysis (XRD). The structure of the second (also unexpected) by-product, new low-dimensional hybrid perovskite $\{Ca(DMF)_6[PbBr_3]_2\}_n$ (**II**) formed in a minor amount (<1 mg) as pale yellow needle-like crystals, was also confirmed by the XRD data. Our attempts to purposefully synthesize this compound from various calcium salts resulted in the discovery of another new low-dimensional hybrid perovskite $\{Ca(DMF)_6[PbBr_{2.3}Cl_{0.7}]_2\}_n$ (**III**).

EXPERIMENTAL

All procedures were carried out in air using commercially available organic solvents distilled in an argon atmosphere. Anthracene and lead(II) bromide (Sigma-Aldrich) were used as received. 7,7,8,8-Tetracyanoquinodimethane was preliminarily recrystallized from its solution in ethyl acetate at 0°C. Anthracen-9-ylmethanamine and anthracen-9-ylmethanamine hydrobromide were synthesized using a modified procedure (Scheme 1) [33]. Analyses of the contents of carbon, nitrogen, and hydrogen were carried out on a Carlo Erba microanalyzer (model 1106).

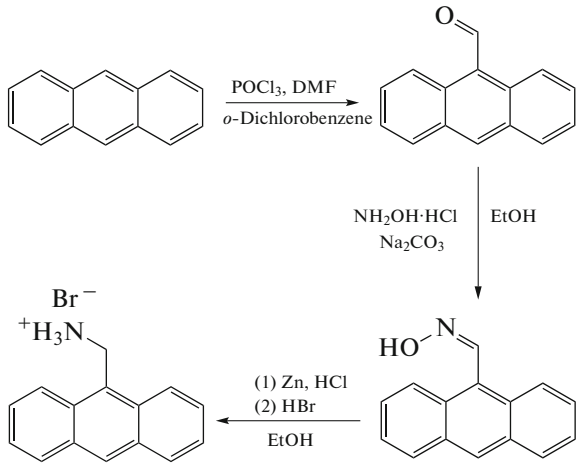

Scheme 1.

Synthesis of anthracene-9-carbaldehyde. DMF (120 mL), phosphorus oxychloride (10.5 mL, 0.23 mol), *o*-dichlorobenzene (10 mL), and anthracene (11.25 g, 0.065 mol) were placed in a round-bottom flask equipped with a magnetic stirrer and a reflux condenser. The mixture was heated to 90–95°C with stirring for 20 min until anthracene was completely dissolved to form a dark red solution with hydrogen chloride evolution. Then heating was continued for 1 h more, after which the solution was neutralized with a saturated aqueous solution of sodium acetate. The resulting mixture was left to stay at −5°C for 2 h. The formed solid residue was crushed, filtered, and washed with distilled water (300 mL). An unpurified solid substance was recrystallized in hot glacial acetic acid. The yield was 10.18 g (76%).

^{1}H NMR (400 MHz, $CDCl_3$), δ, ppm: 7.51 (t, J = 10 Hz, 7-H and 2-H, 2H), 7.64 (t, J = 7.5 Hz, 3-H and 6-H, 2H), 8.00 (d, J = 7.5 Hz, 4-H and 5-H, 2H), 8.72 (s, 10-H, 1H), 9.01 (d, J = 10 Hz, 8-H and 1-H, 2H), 11.45 (s, CHO, 1H). ^{13}C NMR (100 MHz, $CDCl_3$), δ, ppm: 123.46, 124.52, 125.63, 129,09, 125.25, 130.95, 132.04, 135.24, 192.98.

Synthesis of anthracene-9-carbaldehyde oxime. Anthracene-9-carbaldehyde (2 g, 9.64 mmol) and hydroxylamine hydrochloride (0.742 g, 10.66 mmol) were placed in a round-bottom flask with a magnetic stirrer. Ethanol (25 mL) and sodium carbonate (2.055 g, 19.39 mmol) were added. The resulting mixture was stirred at room temperature for 24 h, after which the solvent was evaporated and the residue was washed with distilled water to remove inorganic substances and recrystallized from ethanol. The yield was 1.73 g (81%).

^{1}H NMR (400 MHz, $CDCl_3$), δ, ppm: 7.51 (m, 2-H, 3-H, 6-H, 7-H, 4H), 8.00 (d, J = 8.0 Hz, 4-H and 5-H, 2H), 8.40 (d, J = 5 Hz, 1-H and 8-H, 2H),

8.48 (s, 10-H, 1H), 9.18 (s, CHO, 1H). ^{13}C NMR (100 MHz, $CDCl_3$), δ, ppm: 124.91, 125.41, 126.45, 126.82, 128.87, 129.37, 130.17, 131.24, 148.80.

Synthesis of anthracen-9-ylmethanamine hydrobromide. Hydrochloric acid (12 M, 3.26 mL) and zinc powder (1.6 g, 24.5 mmol) were added to a solution of anthracene-9-carbaldehyde oxime (2.16 g, 9.8 mmol) in ethanol (100 mL), and the mixture was stirred at room temperature for 15 min. Then solutions of ammonia (30%, 2.8 mL) and sodium hydroxide (6 M, 6 mL) were added. The resulting mixture was stirred for 15 min more. The precipitate was filtered off and rejected, and the filtrate was extracted with dichloromethane and dried over anhydrous sodium sulfate. The solvent was evaporated on a rotary evaporator. The dry residue was dispersed in hydrobromic acid (10 mL), filtered off, and washed with a minor amount of ethyl acetate. The obtained precipitate was dried under deep vacuum. The yield was 1.32 g (47%).

^{1}H NMR (400 MHz, DMSO-d_6), δ, ppm: 5.06 (d, J = 5.9 Hz, CH_2, 2H), 7.58 (t, J = 8.0 Hz, 7-H and 2-H, 2H), 7.67 (t, J = 8.0 Hz, 3-H and 6-H, 2H), 8.16 (d, J = 8.6 Hz, 1-H and 8-H, 2H), 8.32 (br.s, NH_3Br, 3H), 8.41 (d, J = 9.0 Hz, 4-H and 5-H, 2H), 8.75 (s, 10-H, 1H). ^{13}C NMR (100 MHz, DMSO-d_6), δ, ppm: 34.81, 124.55, 125.31, 125.96, 127.42, 129.56, 129.73, 130.62, 131.35.

Synthesis of $\{PbBr_2(DMF)\}_n$ (I). Anthracen-9-ylmethanamine hydrobromide (7 mg), lead bromide (8.9 mg), and 7,7,8,8-tetracyanoquinodimethane (5 mg) were dissolved in DMF in a 2-mL glass vial for crystallization. The gas diffusion of diethyl ether to the resulting solution resulted in the formation of transparent needle-like crystals of the product. The yield was 10 mg (64%).

For $C_3H_7NOBr_2Pb$

Anal. calcd., %	C, 8.19	H, 1.60	N, 3.18
Found, %	C, 8.31	H, 1.68	N, 3.22

Synthesis of $\{Ca(DMF)_6[PbBr_3]_2\}_n$ (II). Anthracen-9-ylmethanamine hydrobromide (7 mg), lead bromide (8.9 mg), and 7,7,8,8-tetracyanoquinodimethane (5 mg) were dissolved in DMF in a 2-mL glass vial for crystallization. The gas diffusion of diethyl ether to the resulting solution afforded pale yellow needle-like crystals. The yield was <1 mg.

Synthesis of $\{Ca(DMF)_6[PbBr_{2.3}Cl_{0.7}]_2\}_n$ (III). Lead bromide (8.9 mg) and calcium chloride (2.6 mg) were dissolved in DMF (0.2 mL) with two droplets of acetic acid in a 2-mL glass vial for crystallization. The gas diffusion of diethyl ether to the resulting solution afforded transparent needle-like crystals. The yield was 23 mg (73%).

For $C_{18}H_{42}N_6O_6Cl_{1.39}Br_{4.61}CaPb_2$

Anal. calcd., %	C, 16.50	H, 3.23	N, 6.41
Found, %	C, 17.65	H, 3.71	N, 6.9

XRD of single crystals of compounds **I**–**III** was carried out on a Bruker APEX2 DUO CCD diffractometer (MoK_α radiation, graphite monochromator, ω scan mode). The structures were solved using the ShelXT program [34] and refined in full-matrix least squares using the Olex2 program [35] in the anisotropic approximation for F^2_{hkl}. The positions of hydrogen atoms were geometrically calculated and refined in the isotropic approximation by the riding model. Selected crystallographic data and structure refinement parameters are presented in Table 1.

The structural data for compounds **I**–**III** were deposited with the Cambridge Crystallographic Data Centre (CIF files CCDC nos. 2045586, 2047219, and 2047220, respectively; http://www.ccdc.cam.ac.uk/).

RESULTS AND DISCUSSION

Anthracen-9-ylmethanamine was chosen as the organic donor for the formation a charge-transfer complex in the composition of target hybrid perovskite based on lead bromide. Anthracen-9-ylmethanamine was synthesized using the modified procedure (Scheme 1) [33] from anthracene by the Vilsmeier–Haack formylation with the formation of anthracene-9-carbaldehyde and reduction of the corresponding aldoxime with zinc in hydrochloric acid and washing of the resulting product with hydrobromic acid. Although two latter reactions can be carried out in one step, this is conjugated with a decrease in the yield from 47 to 19%.

7,7,8,8-Tetracyanoquinodimethane is often used for these purposes and, hence, was chosen as the organic acceptor. 7,7,8,8-Tetracyanoquinodimethane was mixed with the synthesized by us anthracen-9-ylmethanamine hydrobromide and lead bromide in equimolar amounts in a suitable solvent. For example, the highest solubility of lead bromide is observed in DMF, dimethyl sulfoxide, and glycerol. However, the attempts to prepare the corresponding perovskite by the liquid diffusion of diethyl ether or dichloromethane from solutions of the indicated reagents in glycerol or dimethyl sulfoxide finished by the formation of oily products. On the contrary, the use of DMF after a prolonged (about 24 days) storage of the reaction mixture in a glass vial for crystallization resulted in the formation of needle-like crystals of two types differed in

Table 1. Selected crystallographic data and structure refinement parameters for compounds **I**–**III**

Parameter	Value		
	I	**II**	**III**
Empirical formula	$C_3H_7NOBr_2Pb$	$C_{18}H_{42}N_6O_6Br_6CaPb_2$	$C_{18}H_{42}N_6O_6Cl_{1.39}Br_{4.61}CaPb_2$
FW	440.11	1372.49	1310.69
T, K		120	
Crystal system	Monoclinic	Triclinic	Triclinic
Space group	$P2_1/n$	$P\bar{1}$	$P\bar{1}$
Z	4	1	1
a, Å	4.3214(10)	8.656(2)	7.6907(5)
b, Å	17.386(4)	9.915(2)	10.4125(7)
c, Å	11.431(3)	12.002(3)	12.4493(9)
α, deg	90.00	92.254(5)	82.6500(10)
β, deg	93.272(5)	107.019(5)	83.3890(10)
γ, deg	90.00	97.759(5)	76.0660(10)
V, Å^3	857.5(3)	972.5(4)	955.96(11)
ρ_{calc}, g cm^{-3}	3.409	2.344	2.277
μ, cm^{-1}	289.18	149.76	139.79
F(000)	768	634	609
$2\theta_{max}$, deg	54	56	52
Number of measured reflections	13318	18085	13610
Number of independent reflections	1876	4687	3759
Number of reflections with $I > 2\sigma(I)$	1445	3971	3228
Number of refined parameters	75	184	227
R_1	0.0561	0.0294	0.0327
wR_2	0.1281	0.0722	0.0993
GOOF	1.073	1.042	1.055
Residual electron density (max/min), e Å^{-3}	2.375/–2.309	1.697/–1.310	1.674/–2.462

color. According to their XRD data (Table 1), the major transparent crystalline product represented the known compound $\{PbBr_2(DMF)\}_n$ (**I**) [36], which can be considered as a hybrid 1D perovskite [22, 28] based on lead bromide forming in the crystal 1D infinite doubled chains with organic solvent molecules that build up the coordination sphere of the lead ion to a distorted octahedron (Table 2, Fig. 1).

Table 2. Selected geometric parameters for compound **I** according to the XRD data at 120 K*

Parameter	**I**
Pb(1)–Br(1), Å	3.0502(17)–3.2220(18)
Pb(1)–Br(2), Å	2.9789(18)–2.9804(17)
Pb(1)–O(1S), Å	2.402(11)
S(OC-6)	1.442

* S(OC-6) is the deviation of the shape of the $PbBr_5O$ coordination polyhedron from an ideal octahedron (OC-6).

However, the minor pale yellow product isolated only in a minor amount (<1 mg) turned out to be a new low-dimensional hybrid perovskite $\{Ca(DMF)_6[PbBr_3]_2\}_n$ (**II**), whose structure (Fig. 2) is similar to the earlier synthesized $\{Mg(DMF)_6[PbI_3]_2\}_n$ (**IV**) [37], by the addition of magnesium iodide dietherate to a solution of lead iodide in DMF. As in the case of isostructural compound **IV** or already described 1D perovskites [22, 28] (including those with the charge-transfer complexes [28]), the inorganic moiety of

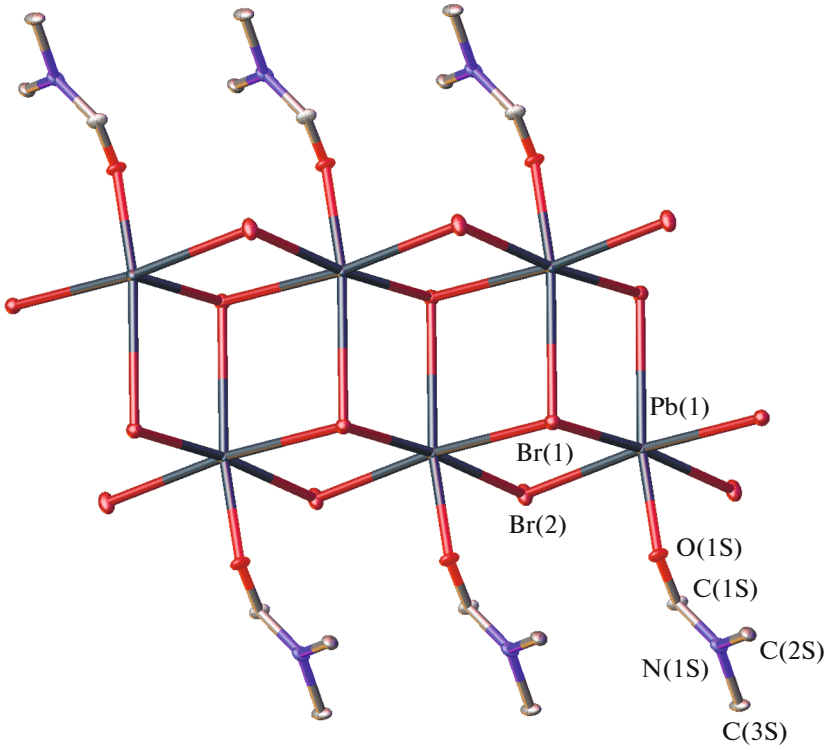

Fig. 1. Fragment of the crystalline packing of 1D perovskite **I** illustrating the formation of infinite chains of lead bromide. Hydrogen atoms are omitted for clarity.

complex **II** represents 1D-infinite chains along the crystallographic axis *a* (Fig. 3) formed by lead(II) cations with three symmetrically nonequivalent bromide anions (Pb–Br 2.7212(8)–3.1333(8) Å), two of which act as bridging ligands (Table 3). As a result, the coordination environment of the lead ion can be characterized as square-pyramidal [9] proposed for the mentioned above compound **IV**, or it can be octahedral with one vacant vertex. This can be determined more reliably using the so-called "continuous symmetry measures" [38] that quantitatively characterize the deviation of the shape of the coordination polyhedron of the metal ion from an ideal square pyramid (SPY-5) or an octahedron with one vacant vertex (vOC-5). The lower the values of these measures, the closer the coordination polyhedron shape to the corresponding polyhedron. For the lead ion in the crystal of compound **II**, the symmetry measures S(SPY-5) and S(vOC-5) estimated from the low-temperature XRD data using the Shape 2.1 program [38] are 1.090 and 0.451, respectively (Table 3). Therefore, its coordination environment should be considered as an octahedron with one vacant vertex (vOC-5). For comparison, the symmetry measure corresponding to the deviation

Table 3. Selected geometric parameters for compound **II** according to the XRD data at 120 K*

Parameter	**II**
Pb(1)–Br(1), Å	2.7212(8)
Pb(1)–Br(2)/Pb(1)–Br(2*A*), Å	3.0129(7)/3.1333(8)
Pb(1)–Br(3)/Pb(1)–Br(3*A*), Å	2.9727(8)/3.0602(7)
Ca(1)–O(1S), Å	2.286(4)
Ca(1)–O(2S), Å	2.273(4)
Ca(1)–O(3S), Å	2.277(4)
S(SPY-5)	1.090
S(vOC-5)	0.451
S(TBPY-5)	6.344
S(OC-6)	0.125

* The Br(2*A*) and Br(3*A*) are symmetric equivalents of the Br(2) and Br(3) atoms obtained by the symmetry transform $-x, -y, -z$. S(SPY-5), S(vOC-5), and S(TBPY-5) are the deviations of the shape of the $PbBr_5$ coordination polyhedron from an ideal square pyramid (SPY-5), an ideal octahedron with one vacant vertex (vOC-5), and an ideal trigonal bipyramid S(TBPY-5), respectively. S(OC-6) is the deviation of the shape of the CaO_6 coordination polyhedron from an ideal octahedron (OC-6).

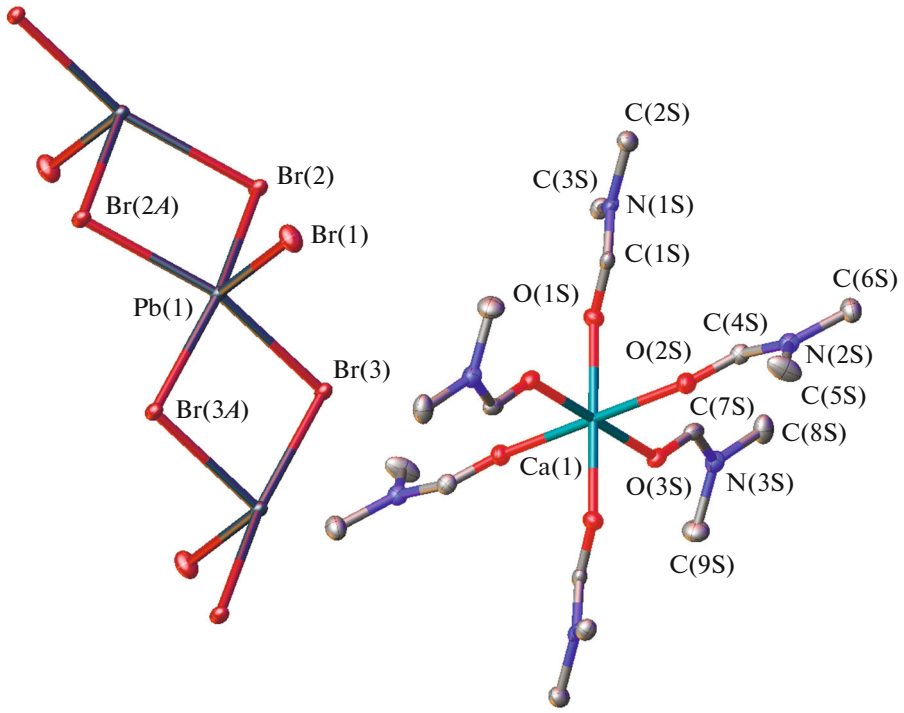

Fig. 2. General view of 1D perovskite **II** in the representation of atoms by thermal vibration ellipsoids ($p = 50\%$). Hydrogen atoms are omitted, and the numeration of atoms is presented only for the symmetrically independent part of the unit cell.

from another ideal coordination polyhedron with five vertices (trigonal bipyramid TBPY-5) takes a much higher value of 6.344.

The calcium cations coordinated by the DMF molecules (Ca–O 2.273(4)–2.286(4) Å) at the vertices of an almost ideal octahedron (Fig. 2) between the 1D chains $\{PbBr_3\}_n$ of the corresponding $PbBr_5$ octahedra with one vacant vertex in the crystal of compound **II** (Fig. 3), which is confirmed by the octahedral symmetry measure S(OC-6) equal to 0.125 (Table 3). The indicated $Ca(DMF)_6^{2+}$ cations are packed into infinite layers perpendicular to the crystallographic axis *c* (Fig. 4) with two coordinated DMF molecules, which separate the neighboring chains $\{PbBr_3\}_n$ thus preventing the formation of the perovskite structure of a higher dimensionality (Fig. 3).

Two most probable reasons for the appearance of calcium ions leading to the formation of hybrid 1D perovskite **II** can be the material of the glass vessel for crystallization (the material could contain, for example, calcium carbonate incorporated in limestone applied for glass fabrication) or water used for washing this vessel after the previous attempt to synthesize hybrid perovskite with 7,7,8,8-tetracyanoquinodimethane and anthracen-9-ylmethanamine hydrobromide. To answer this question, we attempted to reproduce the synthesis of the obtained by us products **I** and **II** under the same conditions when storing the reaction mixture in DMF for the same time (24 days) in another glass vial for crystallization, which was not used earlier. As a result, only one type (transparent) of needle-like crystals was formed corresponding to the known [36] low-dimensional perovskite **I** according to the elemental analysis and XRD data. No pale yellow crystals of hybrid 1D perovskite were observed in the reaction products.

The attempts to purposefully synthesize compound **II** from various calcium salts (nitrate, acetate, sulfate, and chloride) as sources of this metal ions were also unsuccessful. When equimolar amounts of lead bromide and calcium acetate or nitrate, which demonstrated a satisfactory solubility in DMF, were mixed, only the above described low-dimensional perovskite **I** was formed. However, this result was not achieved in the presence of calcium sulfate because of its very low solubility in this solvent. The addition of another solvent, such a glycerol, for a better solubility of all reagents made it possible to dissolve the starting calcium sulfate, but the further attempts of crystallization in this solution gave oily products. The use of a DMF–

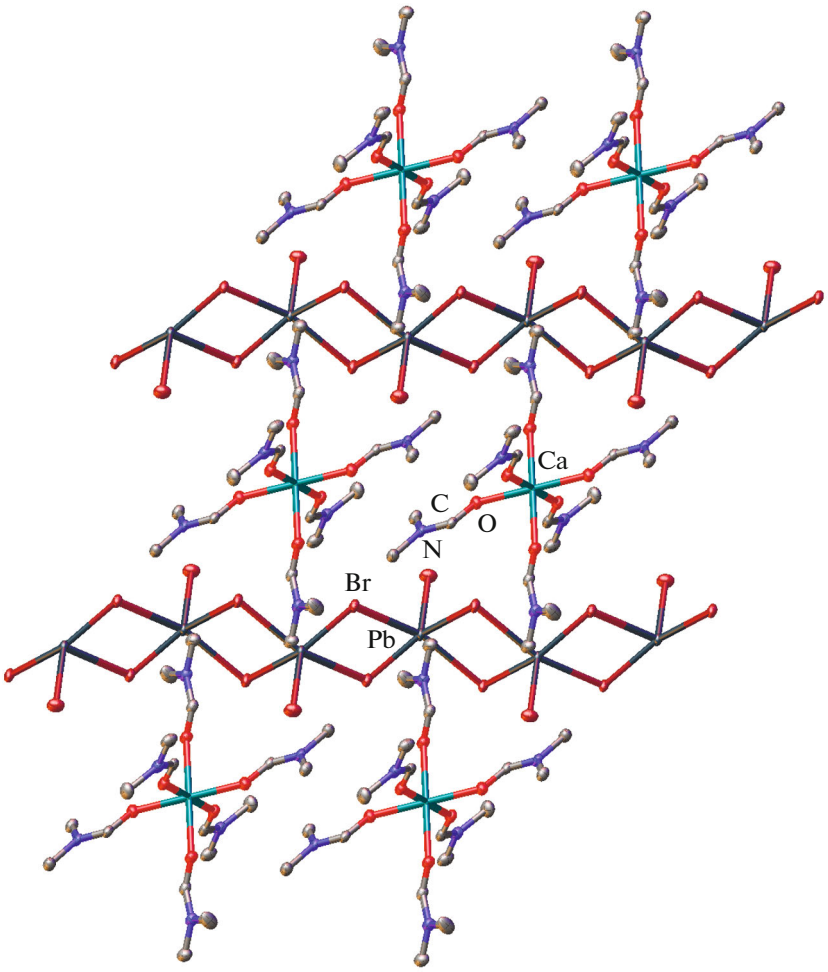

Fig. 3. Fragment of the crystal packing of 1D perovskite **II** illustrating the formation of infinite chains of lead bromide. Hydrogen atoms are omitted for clarity.

acetic acid mixture of solvents for these purposes led to a similar result.

On the contrary, the choice of calcium chloride as the source of calcium ions made it possible to obtain one more hybrid perovskite: $\{Ca(DMF)_6[PbBr_{2.3}Cl_{0.7}]_2\}_n$ (**III**) (Fig. 5), which was isolated in the individual state and characterized by elemental analysis and XRD. According to the XRD results, perovskite **III** differs from the target product **II** by the presence of the chloride anion in the inorganic moiety, and this anion exists in the same position with the Br(3) bromide anion in a ratio of 70 : 30. This results in the formation along the crystallographic axis *a* of 1D-infinite chains $\{PbBr_{2.3}Cl_{0.7}\}_n$ (Fig. 6) in which the chloride or bromide anion builds up the coordination sphere of the lead ion (existing in compound **II** as an octahedron with one vacant vertex) to a nearly ideal octahedron (Pb–Br 2.87(3)–3.0343(11), Pb–Cl 2.91(3)–2.97(3) Å), as follows from the octahedral symmetry measures ranging from 0.827 to 0.944 (Table 4). For comparison, the corresponding value in the above described low-dimensional perovskite **I** is 1.442 (Table 2). Interestingly, a similar change in the structure of the inorganic moiety of hybrid perovskite **III** over that in perovskite **II** does not noticeably change the crystal packing (Figs. 4 and 6). The exception is some distortion of the coordination environment of the calcium ion formed by six DMF molecules, four of which are disordered over two positions due to which the octahedral symmetry measure reaches 0.944.

Thus, we synthesized and characterized the new hybrid low-dimensional perovskite $Ca(DMF)_6[PbBr_3]_2$ (**II**) obtained upon the storage in air of a DMF solution of lead bromide, 7,7,8,8-tetracyanoquinodimethane, and anthracen-9-ylmethanamine hydrobromide in a glass vessel for crystallization. In

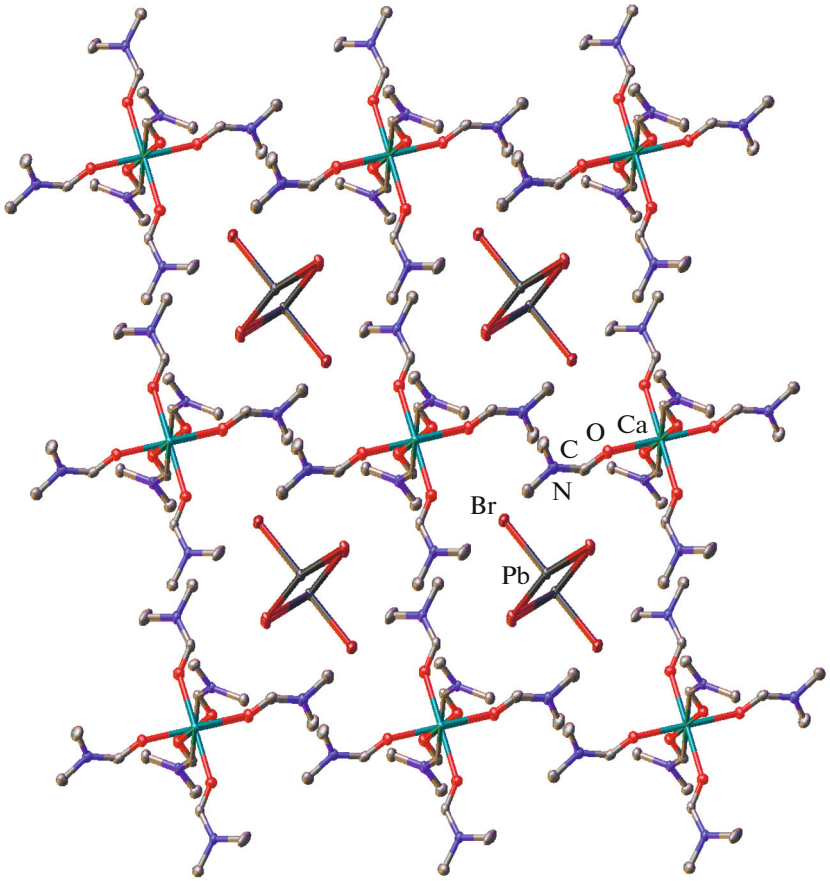

Fig. 4. Fragment of the crystal packing of 1D perovskite **II** illustrating the formation of infinite layers by the $[Ca(DMF)_6]^{2+}$ cations. Hydrogen atoms are omitted for clarity.

Table 4. Selected geometric parameters for compound **III** according to the XRD data at 120 K*

Parameter	**III**
Pb(1)–Br(1), Å	3.0343(11)
Pb(1)–Br(2), Å	3.0193(9)
Pb(1)–Br(3)/Pb(1)–Br(3*A*), Å	2.87(3)/2.94(3)
Pb(1)–Cl(1)/Pb(1)–Cl(1*A*), Å	2.97(3)/2.91(3)
Ca(1)–O(1S), Å	2.288(5)
Ca(1)–O(2S)/Ca(1)–O(2S'), Å	2.308(7)/2.35(2)
Ca(1)–O(3S)/Ca(1)–O(3S'), Å	2.348(13)/2.33(3)
S(OC-6)	0.240–0.944

* The O(2S') and O(3S') atoms belong to the minor component of the disordered DMF molecules. The Br(3*A*) and Cl(1*A*) atoms are symmetric equivalents of the Br(3) and Cl(1) atoms obtained by the symmetry transform $-x, -y, -z$. S(OC-6) is the deviation of the shapes of the PbX_6 and CaO_6 coordination polyhedra from an ideal octahedron (OC-6).

the crystals of this by-product, lead bromide is observed as 1D-infinite chains $\{PbBr_3\}_n$ of the $PbBr_5$ octahedra with one vacant vertex and separated by the calcium cations coordinated with the DMF molecules. The calcium cations presumably got into the reaction mixture from water used for washing of the vessel after the previous attempt of synthesis. Although a more thorough preparation of such reusable vessels allows one, in the most part of cases, to solve this problem, the obstacle can completely be eliminated only on going to nonrecoverable laboratory glassware fabricated, for example, using the additive technology of 3D printing [39]. In the case of calcium chloride, the attempt of the purposeful synthesis of hybrid 1D perovskite **II** from various metal salts expectedly resulted in one more hybrid perovskite: $\{Ca(DMF)_6[PbBr_{2.3}Cl_{0.7}]_2\}_n$ (**III**). Perovskite **III** differs from perovskite **II** by the presence of the chloride anion in the inorganic moiety looking like a 1D-infinite chain $\{PbBr_{2.3}Cl_{0.7}\}_n$ in which the coordination sphere of the lead ion is built up to the octahedral one without appreciable changes in the crystal packing.

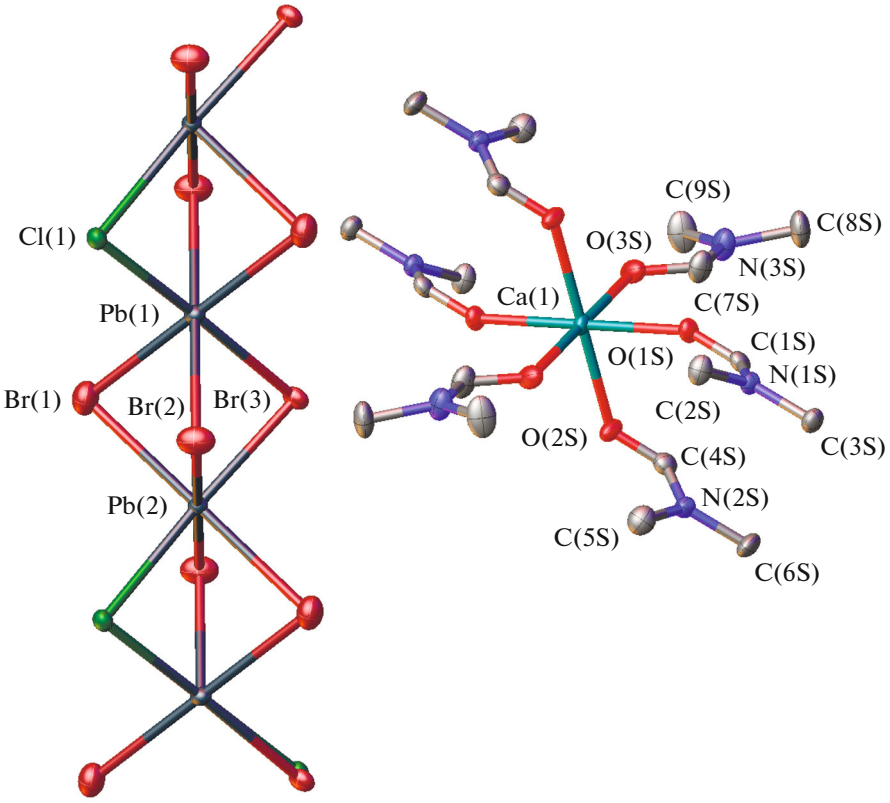

Fig. 5. General view of 1D perovskite **III** in the representation of atoms by thermal vibration ellipsoids ($p = 50\%$). Hydrogen atoms and the minor component of the disordered DMF molecules are omitted, and the numeration of atoms is presented only for the symmetrically independent part of the unit cell.

Unfortunately, under these conditions, we failed to obtain the target low-dimensional perovskite based on lead bromide and containing the charge-transfer complex with anthracen-9-ylmethanamine hydrobromide and 7,7,8,8-tetracyanoquinodimethane as the organic donor and acceptor, respectively. Among the most probable reasons is the steric effect of the bulky anthracenyl fragment remote from the ammonium group at one methylene group only and thus possibly preventing the binding of the group with the inorganic moiety or the steric effect of the alkylammonium substituent impeding the approach of 7,7,8,8-tetracyanoquinodimethane to the π-system of the anthracenyl fragment. In addition, this can also be the electronic effect of the ammonium group due to which the anthracenyl fragment can be an insufficiently good acceptor for the chosen organic donor. The listed reasons are indicated, in particular, by the earlier demonstrated possibility of "self-assembling" of low-dimensional 1D and 2D perovskites [31, 32] under similar conditions but using polyaromatic amine with a longer alkyl chain: 4-pyrenebutanamine. However, the problem of a low solubility of anthracen-9-ylmethanamine hydrobromide in DMF cannot be excluded. The problem can be solved by choosing an alternative solvent or cosolvent (e.g., methanol) and/or by the introduction of the donor and acceptor in the reaction with lead bromide as the prepared beforehand concentrated solution in which they have already formed a charge-transfer complex (for example, according to the optical spectroscopy data).

ACKNOWLEDGMENTS

Elemental analyses were supported by the Ministry of Science and Higher Education of the Russian Federation using the scientific equipment of the Center of Molecular Structure Investigation at the Nesmeyanov Institute of Organoelement Compounds (Russian Academy of Sciences).

FUNDING

This work was supported by the Russian Foundation for Basic Research, project no. 20-33-70052.

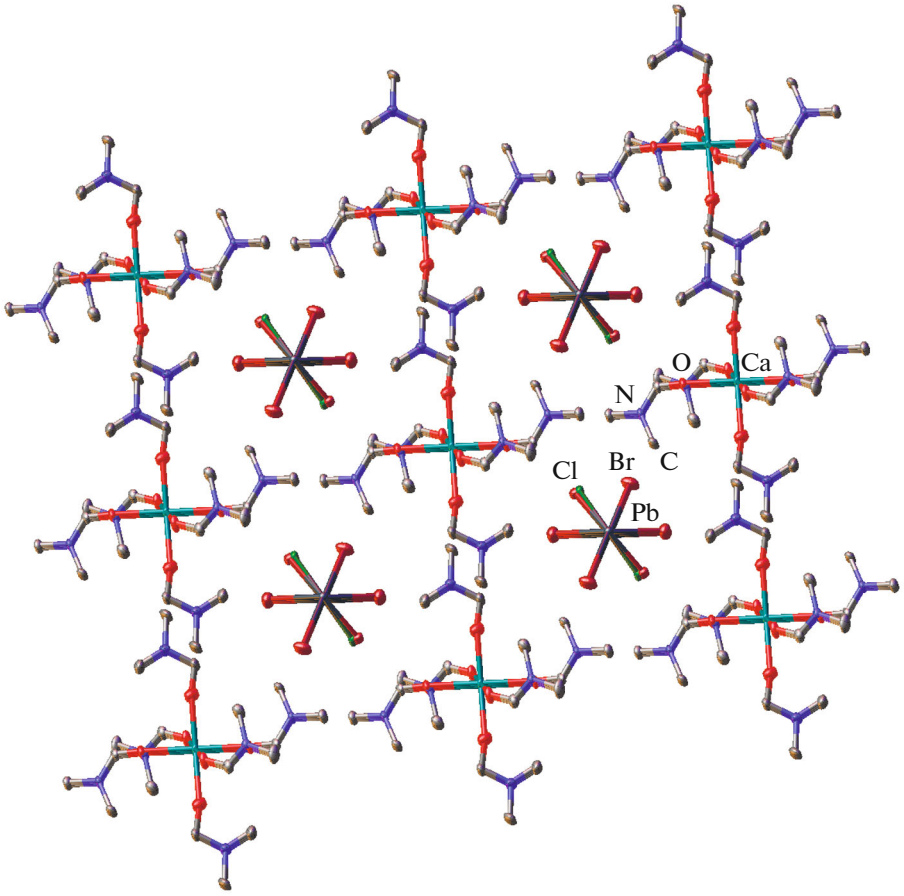

Fig. 6. Fragment of the crystal packing of 1D perovskite **III** illustrating the formation of infinite layers by the $[Ca(DMF)_6]^{2+}$ cations. Hydrogen atoms are omitted for clarity.

CONFLICT OF INTEREST

The authors declare that they have no conflicts of interest.

REFERENCES

1. Kojima, A., Teshima, K., Shirai, Y., and Miyasaka, T., *J. Am. Chem. Soc.*, 2009, vol. 131, no. 17, p. 6050.
2. Jena, A.K., Kulkarni, A., and Miyasaka, T., *Chem. Rev.*, 2019, vol. 119, no. 5, p. 3036.
3. Liu, C., Hu, M., Zhou, X., et al., *NPG Asia Mater.*, 2018, vol. 10, no. 6, p. 552.
4. Hong, K., Le, Q.V., Kim, S.Y., and Jang, H.W., *J. Mat. Chem. C*, 2018, vol. 6, no. 9, p. 2189.
5. Niu, T., Ren, H., Wu, B., et al., *J. Phys. Chem. Lett.*, 2019, vol. 10, no. 10, p. 2349.
6. Misra, R.K., Cohen, B.-E., Iagher, L., and Etgar, L., *ChemSusChem*, 2017, vol. 10, no. 19, p. 3712.
7. Zhang, J., Yang, X., Deng, H., et al., *Nano-Micro Lett.*, 2017, vol. 9, no. 3, p. 36.
8. Zhou, C., Lin, H., He, Q., et al., *Mater. Sci. Eng. Reports*, 2019, vol. 137, p. 38.
9. Zhou, C., Worku, M., Neu, J., et al., *Chem. Mater.*, 2018, vol. 30, no. 7, p. 2374.
10. Xu, L.-J., Sun, C.-Z., Xiao, H., et al., *Adv. Mater.*, 2017, vol. 29, no. 10, p. 1605739.
11. Huo, C., Cai, B., Yuan, Z., et al., *Small Methods*, 2017, vol. 1, no. 3, p. 1600018.
12. Smith, I.C., Hoke, E.T., Solis-Ibarra, D., et al., *Angew. Chem., Int. Ed. Engl.*, 2014, vol. 53, no. 42, p. 11232.
13. Saparov, B. and Mitzi, D.B., *Chem. Rev.*, 2016, vol. 116, no. 7, p. 4558.
14. Kieslich, G., Sun, S., and Cheetham, A.K., *Chem. Sci.*, 2015, vol. 6, no. 6, p. 3430.
15. Travis, W., Glover, E.N.K., Bronstein, H., et al., *Chem. Sci.*, 2016, vol. 7, no. 7, p. 4548.
16. Grancini, G. and Nazeeruddin, M.K., *Nature Rev. Mater.*, 2019, vol. 4, no. 1, p. 4.
17. He, T., Li, S., Jiang, Y., et al., *Nat. Commun.*, 2020, vol. 11, no. 1, p. 1672.
18. Lan, C., Zhou, Z., Wei, R., and Ho, J.C., *Materials Today Energy*, 2019, vol. 11, p. 61.
19. Zhang, F., Lu, H., Tong, J., et al., *Energy Environ. Sci.*, 2020, vol. 13, no. 4, p. 1154.
20. Mao, L., Stoumpos, C.C., and Kanatzidis, M.G., *J. Am. Chem. Soc.*, 2019, vol. 141, no. 3, p. 1171.
21. Mousdis, G.A., Gionis, V., C. Papavassiliou, G., et al., *J. Mat. Chem.*, 1998, vol. 8, no. 10, p. 2259.

22. Ma, C., Shen, D., Huang, B., et al., *J. Mat. Chem. A*, 2019, vol. 7, no. 15, p. 8811.
23. Zhou, C., Tian, Y., Wang, M., et al., *Angew. Chem., Int. Ed. Engl.*, 2017, vol. 56, no. 31, p. 9018.
24. Yin, J., Maity, P., De Bastiani, M., et al., *Sci. Adv.*, 2017, vol. 3, no. 12, p. e1701793.
25. Zhou, C., Lin, H., Lee, S., Chaaban, M., and Ma, B., *Mat. Res. Lett.*, 2018, vol. 6, no. 10, p. 552.
26. Passarelli, J.V., Fairfield, D.J., Sather, N.A., et al., *J. Am. Chem. Soc.*, 2018, vol. 140, no. 23, p. 7313.
27. Van Gompel, W.T.M., Herckens, R., Van Hecke, K., et al., *Chem. Commun.*, 2019, vol. 55, no. 17, p. 2481.
28. Marchal, N., Van Gompel, W., Gelvez-Rueda, M.C., et al., *Chem. Mater.*, 2019, vol. 31, no. 17, p. 6880.
29. Evans, H.A., Lehner, A.J., Labram, J.G., et al., *Chem. Mater.*, 2016, vol. 28, no. 11, p. 3607.
30. Maughan, A.E., Kurzman, J.A., and Neilson, J.R., *Inorg. Chem.*, 2015, vol. 54, no. 1, p. 370.
31. Goetz, K.P., Vermeulen, D., Payne, M.E., et al., *J. Mater. Chem. C*, 2014, vol. 2, no. 17, p. 3065.
32. Jiang, H., Hu, P., Ye, J., et al., *J. Mat. Chem. C*, 2018, vol. 6, no. 8, p. 1884.
33. Ayedi, M.A., Le Bigot, Y., Ammar, H., et al., *Synth. Commun.*, 2013, vol. 43, no. 16, p. 2127.
34. Sheldrick, G.M., *Acta Crystallogr., Sect. A: Found. Crystallogr.*, 2008, vol. 64, p. 112.
35. Dolomanov, O.V., Bourhis, L.J., Gildea, R.J., et al., *J. Appl. Crystallogr.*, 2009, vol. 42, p. 339.
36. Liu, M., Zhao, J., Luo, Z., et al., *Chem. Mater.*, 2018, vol. 30, no. 17, p. 5846.
37. Krautscheid, H. and Vielsack, F., *Z. Anorg. Allg. Chem.*, 1999, vol. 625, p. 562.
38. Alvarez, S., *Chem. Rev.*, 2015, vol. 115, p. 13447.
39. Zalesskiy, S.S., Kitson, P.J., Frei, P., et al., *Nat. Commun.*, 2019, vol. 10, p. 5496.

Translated by E. Yablonskaya